Journal of Engineering Science and Technology
Vol. 13, No. 9 (2018) 2805 - 2819


# PAPR FOR OFDM SYSTEM BASED ON FAST DISCRETE CURVELET TRANSFORM

MOHAMED H. M. NERMA[1,2,*], MOHAMMED A. A. ELMALEEH[1]

[1]University of Tabuk, Faculty of Computer and Information Technology,
P.O. Box 71491, Tabuk, Kingdom of Saudi Arabia
[2]Sudan University of Science and Technology, College of Engineering,
Khartoum, Sudan
*Corresponding Author: mnerma@ut.edu.sa

## Abstract

Orthogonal Frequency-Division Multiplexing (OFDM) is an attractive transmission technique for high-bit-rate communication systems. However, high Peak to Average Power Ratio (PAPR) of transmitted signals is a major shortcoming for Multi-Carrier Modulation (MCM) system such as the OFDM system. Traditional OFDM implementations use common Fourier filters for data modulation and demodulation via the Inverse Fast Fourier Transform (IFFT) and the FFT operations respectively, in this paper the Fast Discrete Curvelet Transform (FDCT) is proposed for OFDM in order to reduce the PAPR. The software CurveLab, used in this work is available at http://www.curvelet.org. The proposed system used FDCT via both Unequispaced Fast Fourier Transform (USFFT) and Wrapping. In terms of PAPR, the results show that both transforms used in this work gives better PAPR results, FDCT via USFFT and FDCT via Wrapping are given approximately about 7.7 dB reduction compared to traditional OFDM. Moreover, the results show that the BER performance of the considered system nearly matches the theoretical BPSK BER performance in an Additive White Gaussian Noise (AWGN) channel.

Keywords: BER, Curvelet transforms, FFT, OFDM, PAPR, Unequispaced FFT, Wavelet transforms, Wrapping.

## 1. Introduction

Traditional OFDM implementations use common Fourier filters for data modulation and demodulation via the Inverse Fast Fourier Transform (IFFT) and the FFT operations respectively [1-6]. Recent research has demonstrated that improved spectral efficiency can be obtained by using wavelet filters owing to their superior spectral containment properties. This has motivated the design of OFDM systems based on Discrete Wavelet Transform (DWT) [7-18] and Wavelet Packet Transform (WPT) [19-25]. As all the characteristics of OFDM modulated signals directly depend on the set of waveforms arising from using a given wavelet filter, several authors foresaw wavelet theory as a good platform on which, to build OFDM waveform bases.

Moreover, the Dual-Tree Complex Wavelet Transform (DTCWT) is used as a new platform to build a new OFDM system that can meet the stringent requirements of the future wireless communication systems [26-35].

## 2. OFDM System

OFDM is an efficient MCM scheme for wireless, frequency selective communication channels. In the baseband equivalent OFDM transmitter with $N$ subcarriers, $N$ modulation symbols in the $m-th$ data frame, $a^m[k]$ where $k = 0, 1, \ldots, N-1$, are mapped over the interval $[0,T]$ on to the continuous time OFDM signal, $x(t)$, as follows:

$$x(t) = \frac{1}{N}\sum_{k=0}^{N-1} a[k]e^{j2\pi k f_0 t} \qquad t \in [0,T] \tag{1}$$

where $f_0 = 1/T$, $j$ is equal to square root of -1 , $T$ is the symbol duration, and for the brevity of notation, indexing of the frames ($m$) is dropped. Figure 1 shows the OFDM system functional block diagram.

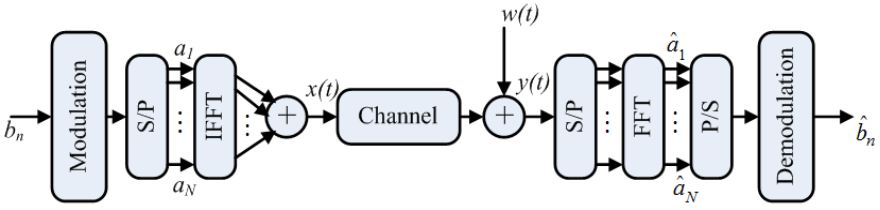


**Fig. 1. Functional block diagram of OFDM system.**

The discrete time version of Eq. (1), referred to as the OFDM frame, is formed by sampling the continuous signal $x(t)$ using the nyquist rate$1/T$ at $N$ time instances such that $t= nT/N$ to get:

$$x(n) = \frac{1}{N}\sum_{k=0}^{N-1} a[k]e^{j2\pi kn/N} \tag{2}$$

where $n$= 0, 1, . . ., $N$-1. In Eq. (2), the OFDM symbols $x[n]$ are related to the modulation symbols $a[k]$ through an Inverse Discrete Fourier Transform (IDFT). When $N$ is a power of two, the IDFT can be evaluated using the computationally efficient IFFT. Figure 1 shows a functional block diagram of an OFDM system. On the receiver side, the FFT is used for decoupling the subcarrier followed by a demodulator to detect the signalling points. The PAPR of the transmitted signals in Eq. (1) is defined as the maximum instantaneous power of the over average power [36, 37].

$$PAPR = \frac{max\{|x[n]|^2\}}{E\{|x[n]|^2\}} \tag{3}$$

where $E\{.\}$ denotes the ensemble average calculated over the duration of the OFDM symbol. Given a specified PAPR threshold, $PAPR_0 = \lambda_0$, the Complementary Cumulative Distribution Function (CCDF) of the PAPR is given as [38, 39]:

$$CCDF(PAPR\{x(t)\}) = P_r(PAPR\{x(t)\} \geq \lambda_0) = 1 - \left(1 - e^{-\lambda_0}\right)^N \tag{4}$$

The BER reduction is another key issue in wireless communication. To measure the noise robustness of OFDM scheme, the relationship of the BER as a function of Energy per Bit to Noise Power Spectral Density Ratio ($E_b/N_0$) for different levels of noise is a useful performance tool.

The BER performance of the OFDM system matches the theoretical BER performance of Binary Phase Shift Keying (BPSK) modulation given as

$$P_e = Q\left(\sqrt{2(E_b/N_o)}\right) \tag{5}$$

## 3. Curvelet Transform

The curvelet was introduced in 2000 [40]. Nowadays the curvelet transform has been applied in various areas including image processing [41-45], seismic processing [46-48], turbulence analysis in fluid mechanics [49-52], solving of Partial Different Equations (PDEs) [53, 54] and Compressed Sensing or Compressive Sampling (CS) [55-59]. The curvelets transform as basis functions are verified in the above works as being effective in many fields. The two simpler, faster, and less redundant FDCTs are used in this work are curvelets via USFFT, and curvelets via wrapping [60].**FDCT via USFFTs**

In the USFFT version, the discrete fourier transform, viewed as a trigonometric polynomial, is sampled within each parallel epipedal region according to an equispaced grid aligned with the axes of the parallelogram. Hence, there is a different sampling grid for each scale/orientation combination. The forward transform is specified in the closed form and is invertible. The software CurveLab for the FDCT [60] used in this work is available at http://www.curvelet.org for academic use. For the vector $x(t)$; $-n/2 \leq t \leq n/2$ of size $n$, with a set of points ($f_k$); $1 \leq k \leq m$. The Fourier Transform (FT) of $x(t)$ is given by:

$$X(f_k) = y[k] = \sum_{t=-n/2}^{n/2} x(t)\, e^{-j2\pi f_k t} \tag{6}$$

The inverse transform takes the form:

$$x(t) = \sum_{k=1}^{m} X(f_k)\, e^{j2\pi f_k t} = \sum_{k=1}^{m} y[k]\, e^{j2\pi f_k t} \tag{7}$$

The problem related to Eqs. (6) and (7) is the computation complexity, using the non-uniform FFT strategy is the one solution. First express $x(t)$ in Eq. (2) as FT of the series of impulse signal as:

$$Y(f) = \sum_{k=1}^{m} y[k]\ \ \delta(f - f_k) \tag{8}$$

The idea is then to convolve $Y(f)$ with a short filter $H(f)$ to make it approximately bandlimited, then to sample the result on a regular grid and apply the FFT, and finally deconvolve the output to correct for the convolution with $H(f)$[61].

The other solution is by using the USFFTs strategy [60], in order to compute the intermediate Fourier samples on a finer grid and to use the Taylor approximations to compute approximate values of $X(f_k)$ at each node $f_k$. The algorithm operates as follows:

Pad the signal $x(t)$ with zeros to create $x^{\wedge}(t)$ of size $Dn$ of-$Dn/2 \leq t \leq Dn/2$:

$$\hat{x}(t) = \begin{cases} x(t) & n/2 \leq t \leq n/2 \\ 0 & elswhere \end{cases} \tag{9}$$

Then make $L$ copies of $x^{\wedge}(t)$ and multiply each copy by $(-it)^l$ to obtaining:

$$\hat{x}^l(t) = (-it)^l \hat{x}(t), \qquad l = 0, 1, 2, \cdots, L-1 \tag{10}$$

Then take the FFT of $x^{\wedge l}(t)$ thus obtain the $X^{\wedge l}(f_k)$ with spacing $2\pi/n$, namely, $X^{\wedge l}(2\pi k/nD)$.

Finally given an arbitrary point $f$, evaluate an approximation of $X(f)$ by

$$X(f) \approx Y(f_0) := X(f_0) + \acute{X}(f_0)(f - f_0) + \cdots + X^{(L-1)}(f_0)\frac{(f - f_0)^{(L-1)}}{(L-1)!} \tag{11}$$

where $f_0$ is the closest fine grid point of $f$.

## 3.2. FDCT via frequency wrapping

In the wrapping version, instead of interpolation, it uses periodization to localize the fourier samples in a rectangular region in which, the IFFT can be applied. For a given scale, this corresponds only to two cartesian sampling grids, one for all angles in the east-west quadrants, and one for the north-south quadrants. The forward transform is specified in the closed form and is invertible with inverse in the closed form.

The curvelet transforms computed by wrapping is as geometrically faithful to the continuous transform as the sampling on the grid allows. The wrapping FDCT implementation is based on the FFT algorithm and the data flow diagram of the

forward and inverse wrapping FDCT are plotted in Fig. 2. The data are first transformed into the frequency domain by forwarding the FFT and then multiplied with a set of window functions. The curvelet coefficients are obtained by inverse FFT (IFFT) from windowing data. Since the window functions are zero except on support regions of elongated wedges, the regions that need to be transformed by the IFFT are much smaller than the original data. On the wrapping FDCT, the FFT coefficients on these regions are 'wrapped' or folded into a rectangular shape before being applied to the IFFT algorithm. The size of the rectangle is usually not an integer fraction of the size of the original data. This process is equivalent to filtering and subsampling the curvelet subband by rational numbers in two dimensions. The complexity of both algorithms for computing $L$ FFTs of length $Dn$ followed by $m$ evaluation of the Taylor polynomial is only of $O$ ($n \log n + m$).

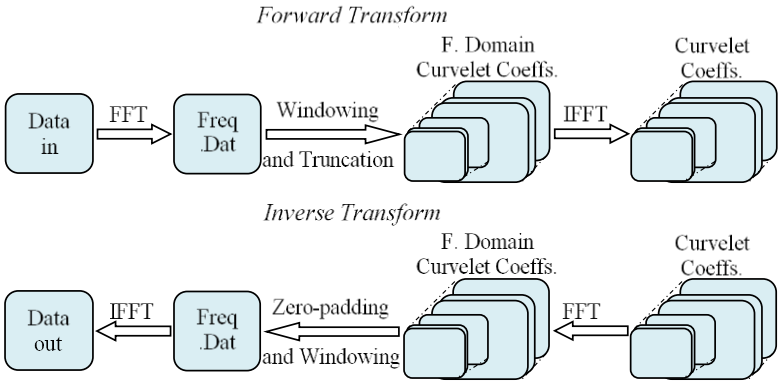


**Fig. 2. Forward and inverse wrapping FDCT.**

## 4. System Model

Similar to the OFDM system based on FFT, a functional block diagram of OFDM based on FDCT is shown in Fig. 3. The FDCT and IFDCT blocks are used at the transmitter and the receiver side respectively.

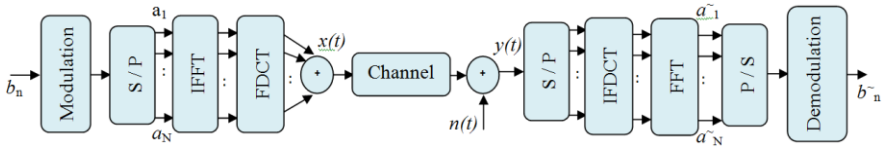


**Fig. 3. Functional block diagram of OFDM system based on FDCT.**

The simulation procedures used in this work were summarized in the flowchart shown in Fig. 4. All the simulation mentioned above are carried out using MATLAB® program using FFT/IFFT and FDCT/IFDCT functions. The simulation of BER carried out in this work in Additive White Gaussian Noise (AWGN). The simulation parameters are documented in Table 1.

The performance of the PAPR of the proposed system is quantified through the simulation. The PAPR results are obtained using the CCDF, the PAPR performance can be illustrated by the CCDF of the PAPR. The system model contains only the

transmitter section in order to evaluate the performance of PAPR using the value of 2 dB threshold as documented in Table 1.

The BER is calculated by comparing the transmitted and the received data in the AWGN channel, the system model includes a transmitter and the receiver side of the flow chain shown in Fig. 4 with an AWGN block in between. The simulations are carried out under the MATLAB® environment.

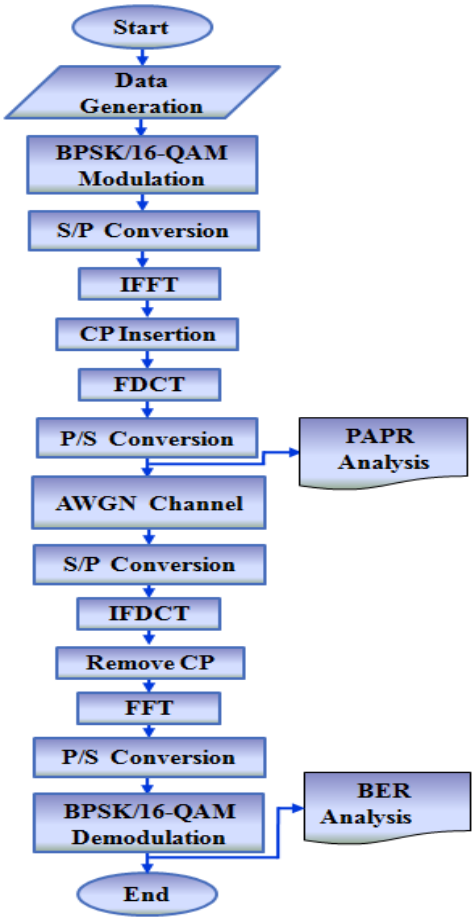


**Fig. 4. Flow chart of the simulation procedures.**

**Table 1. Simulation parameters.**

| Simulation parameters | |
|---|---|
| **Modulation** | BPSK and 16-QAM |
| **Channel** | AWGN |
| **Number of subcarriers (*N*)** | 64 |
| **PAPR threshold** | 2 dB |
| **Cyclic Prefix (CP)** | ¼ |
| **Number of symbols** | 10000 |
| **Number of data subcarriers** | 52 |
| **Number of bits per OFDM symbol** | 52 |

## 5. Results and Discussion

Among the performance metric parameters of the considered system such as PAPR, PSD, the accuracy of channel estimation, computational complexity, data rate, and sensitivity to synchronization, this work will focus on PAPR, BER, and computational complexity. The remaining parameters are planned to be considered in the future work related to this system.

### 5.1. Complementary cumulative distribution function

The CCDF of the transmitter in this proposed system is quantified by the same simulation parameters of the above section with 16-QAM using FDCT via USFFT and FDCT via wrapping. The results obtained are shown in Figs. 5 and 6 respectively. The dashed red curve represents the CCDF of the proposed system while the solid blue curve represents the conventional OFDM. At 0.01% of CCDF, the proposed system has a PAPR of approximately 2.5 dB while the conventional OFDM has a PAPR of approximately 10.2 dB. It is observed that the proposed system achieved 7.7 dB improvements over the conventional OFDM system at 0.01% of CCDF.

In Fig. 6, the first dashed red curve represents the CCDF of the proposed system while the solid blue curve represents the conventional OFDM. At 0.01% of CCDF, the proposed system has a PAPR of approximately 2.4 dB while the conventional OFDM has a PAPR of approximately 10.1 dB. The results showed that the proposed system has achieved 7.7 dB improvements over the conventional OFDM system at 0.01% of CCDF.

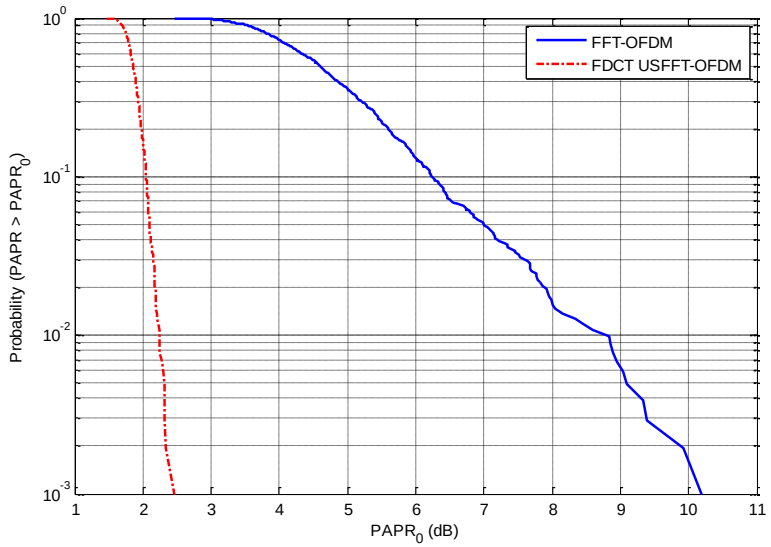


**Fig. 5. CCDF for the OFDM system based on FDCT via USFFT.**

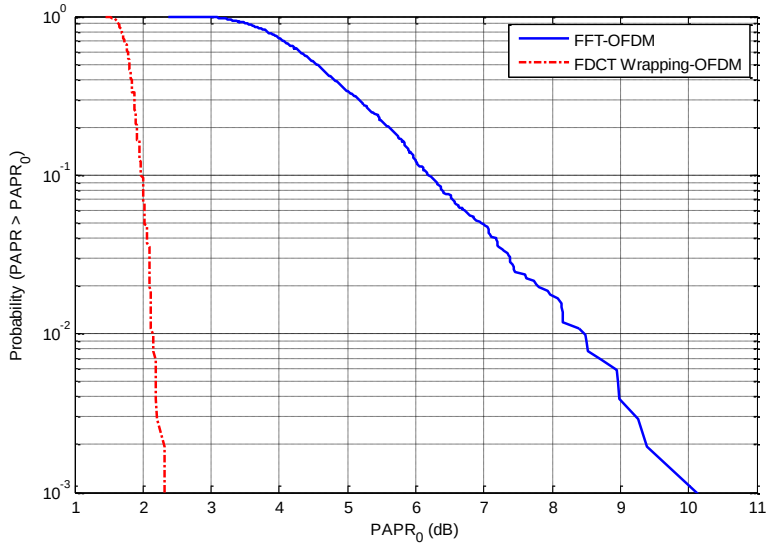


**Fig. 6. CCDF for the OFDM system based on FDCT via wrapping.**

## 5.2. Bit Error Rate

The relationship of the BER as a function of the Energy per Bit to Noise Power Spectral Density Ratio (Eb/No) performance is a useful performance tool, which is used to measure the noise robustness of the proposed system. The results of the BER performance using FDCT via USFFT and FDCT via wrapping are presented in Figs. 7 and 8 respectively.

In the results shown in Figs. 7 and 8, the dotted red curve represents the BER performance of the proposed system; the second dashed black curve represents the BER for conventional OFDM system. The solid blue curve denotes the theoretical BPSK. The results showed that the BER performance of the considered system nearly complies with the theoretical BPSK BER performance in an AWGN channel.

## 5.3. Computational complexity

Computational complexity is an important issue. Due to the high data rates required in modern applications, low complexity is imperative. Computational complexity is considered as one of the drawbacks of the proposed system because Fourier has a computational complexity of $O$ ($n \log n$), where $n$ is the rank of the transform, or the number of subchannels while the FDCT has a computational complexity of $O$ ($n \log n + m$), which means the complexity of the FDCT has higher order compared to the complexity of fourier.

Using laptop processor Pentium (R) Dual-Core CPU 2.2 GHz with 1 GB RAM, both algorithms having the same output, but for calculating the PAPR, the USFFT algorithm take 23.9 seconds elapsed time for the forward FDCT USFFT and 59.2 seconds for the inverse transform while the wrapping algorithm takes only 4.6 seconds elapsed time for the forward transform and 3.2 seconds for the

inverse transform. On the other side for calculating the BER, the USFFT algorithm takes 25 seconds elapsed time for the forward FDCT USFFT and 57.2 seconds for the inverse transform while the wrapping algorithm takes only 2.9 seconds elapsed time for the forward transform and 3.5 seconds for the inverse transform. Thus, that the wrapping algorithm gives a faster computation time as compared to the USFFT algorithm

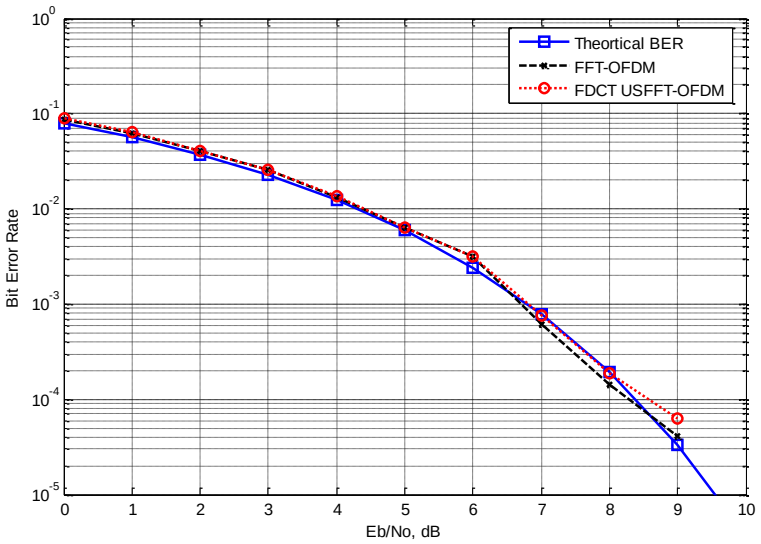


**Fig. 7. BER performance of OFDM system based on FDCT via USFFT.**

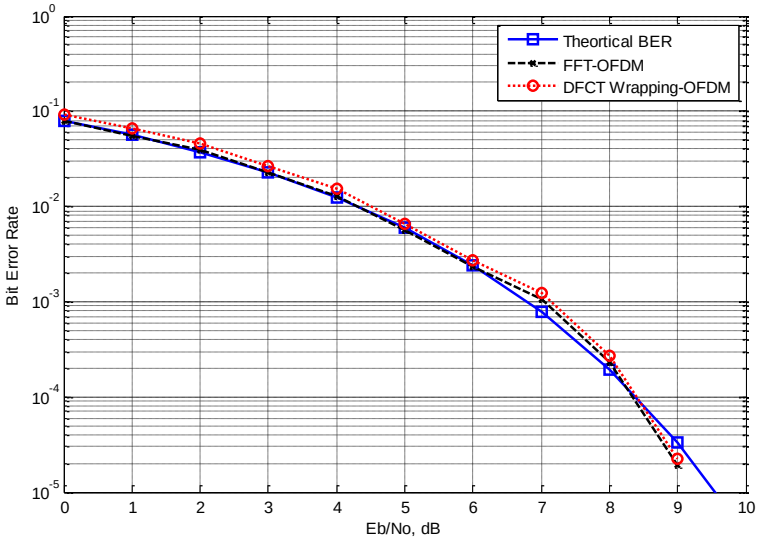


**Fig. 8. BER performance of OFDM system based on FDCT via wrapping.**

## 6. Conclusions

This work has implemented the FDCT to design a new OFDM system. It was demonstrated via the CCDF of the transmitted signal that the proposed system gives better PAPR results compared to the conventional OFDM system. The simulation results also showed that the BER performance in AWGN indicates that the performance of the proposed system nearly matches the theoretical BER performance of BPSK modulation in AWGN channel. Finally, it is observed that the proposed system has more computational complexity compared to the conventional OFDM, which leads to many research opportunities in this area. Some suggestions for the future work include:

- The PAPR reduction techniques can be tested in this system.
- The synchronization techniques could be an area that may be addressed.
- Channel estimation technique in the proposed system can be investigated.
- The effects of the multiple transmit and receive antennas can be explored.
- The computational complexity of this system can also be tested in order to give better results.

### Nomenclatures

| | |
|---|---|
| $f_0$ | Closest fine grid point of $f$ |
| $f_c$ | Carrier frequency |
| $h(t)$ | Channel impulse response |
| $K$ | Translation index |
| $M$ | Scaling index |
| $N$ | No. of subcarriers |
| $PAPR_0$ | PAPR threshold |
| $w(t)$ | AWGN noise |
| $x(t)$ | Continuous time transmitted signal |
| $y(t)$ | Continuous time received signal |

***Greek Symbols***

| | |
|---|---|
| $\sigma^2$ | Noise variance |
| $\lambda^2$ | PAPR threshold ($PAPR_0$) |

**Abbreviations**

| | |
|---|---|
| AWGN | Additive White Gaussian Noise |
| BER | Bit Error Rate |
| BPSK | Binary Phase Shift Keying |
| CCDF | Complementary Cumulative Distribution Function |
| CNR | Carrier to Noise Ratio |
| CP | Cyclic Prefix |
| CS | Compressed Sensing or Compressive Sampling |
| DTDCWT | Dual-Tree Discrete Complex Wavelet Transform |
| DWT | Discrete Wavelet Transform |
| Eb/No | Energy per Bit to Noise Power Spectral Density Ratio |
| FDCT | Fast Discrete Curvelet Transform |
| FFT | Fast Fourier Transform |
| FT | Fourier Transform |

| | |
|---|---|
| IDFT | Inverse Discrete Fourier Transform |
| IFDCT | Inverse Fast Discrete Curvelet Transform |
| IFFT | Inverse Fast Fourier Transform |
| MCM | Multi-Carrier Modulation |
| OFDM | Orthogonal Frequency Division Multiplexing |
| PAPR | Peak to Average Power Ratio |
| PDEs | Partial Different Equations |
| PSK | Phase Shift Keying |
| QAM | Quadrature Amplitude Modulation |
| UFFT | Unequispaced Fast Fourier Transform |
| WPM | Wavelet Packet Modulation |
| WPT | Wavelet Packet Transform |
| WT | Wavelet Transform |

## References


1. Bingham, J.A.C. (2010). Multicarrier modulation for data transmission: An idea whose time has come. *IEEE Communications Magazine*, 28(5), 5-14.
2. Saltzberg, B. (1967). Performance of an efficient parallel data transmission system. *IEEE Transactions on Communication Technology*, 15(6), 805-811.
3. Weinstein, S.; and Ebert, P. (1971). Data transmission by frequency division multiplexing using discrete fourier transform. *IEEE Transactions on Communication Technology*, 19(5), 628-634.
4. Cimini, L. (1985). Analysis and simulation of a digital mobile channel using orthogonal frequency division multiplexing. *IEEE Transactions on Communication*s, 33(7), 665-675.
5. Steendam, H.; and Mcneclaey, M. (1999). Analysis and optimization of the performance of OFDM on frequency-selective time-selective fading channels. *IEEE Transactions on Communication*, 47(12), 1811-1819.
6. Kim, Y.H.; Song, I.; Kim, H.G.; Chang, T.; Kim, H.M. (1999). Performance analysis of a coded OFDM system in time-varying multipath rayleigh channels. *IEEE Transactions on Vehicular Technology*, 48(5), 1610-1615.
7. Newlin, H.M. (1998). Developments in the use of wavelets in communication systems. *Proceedings of the IEEE-Military Communications Conference*. Boston, Massachusetts, United States of America, 343-349.
8. Tzannes, M.A.; Tzannes, M.C; Proakis, J.; and Heller, P.N. (1994). DMT systems, DWMT systems and digital filter banks. *Proceedings of IEEE International Conference on Communications (ICC/SUPERCOMM'94)*. New Orleans, Los Angelas, United States of America, 311-315.
9. Sandberg, S.D.; and Tzannes, M.A. (1995). Overlapped discrete multitone modulation for high speed copper wire communications. *IEEE Journal on Selected Areas in Communications*, 13(9), 1571-1585.
10. Akansu, A.N.; and Lin, X. (1998). A comparative performance evaluation of DMT (OFDM) and DWMT (DSBMT) based DSL communications systems for single and multitone interference. *Proceedings of the IEEE International Conference on Acoustics, Speech and Signal Processing (ICASSP'98)*. Seattle, Washington, United States of America, 3269-3272.

11. Werner, K.; Gotz, P.; Jorn, U.; and Geog, Z. (2000). A comparison of various MCM schemes. *Proceedings of the 5th International OFDM Workshop*. Hamburg, Germany, 20-1-20-5.
12. Zhang, H.; Yuan, D.; Jiang, M.; and Wu, D. (2004). Research of DFT-OFDM and DWT-OFDM on different transmission scenarios. *Proceedings of the 2nd International Conference on Information Technology and Applications (ICITA 2004)*. Harbin, China, 3 pages.
13. Sun, M.C.; and Lun, D.P.K. (2002). Power-Line communications using DWMT modulation. *Proceedings of the IEEE International Symposium on Circuits and Systems*. Phoenix-Scottsdale, Arizona, United States of America, 4-6.
14. Baig, S.; Fazal-ur-Rehman; and Mughal, M.J. (2005). Performance comparison of dft, discrete wavelet packet and wavelet transforms in an OFDM transceiver for multipath fading channel. *Proceedings of the IEEE Pakistan Section Multitopic Conference*. Karachi, Pakistan, 1-6.
15. Gupta, D.; Vats, V.B.; and Garg, K.K. (2008). Performance analysis of DFT-OFDM, DCT-OFDM, and DWT-OFDM systems in AWGN channel. *Proceedings of the 4th International Conference on Wireless and Mobile Communications (ICWMC'08)*. Washington D.C., United States of America, 214-216.
16. Chafii, M.; Palicot, J.; Gribonval, R.; and Burr, A.G. (2016). Power spectral density limitations of the wavelet-OFDM system. *Proceedings of the 24th European Signal Procesing Conference (EUSIPCO)*. Budapest, Hungary, 1428-1432.
17. Chafii, M.; Palicot, J.; and Gribonval, R. (2017). Wavelet modulation: An alternative modulation with low energy conssumption. *Comptes Rendus Physique*, 18(2), 156-167.
18. Damati, A.; Daoud, O.; and Hamarsheh, Q. (2016). Enhancing the odd peaks detection in OFDM using wavelet transforms. *International Journal Communications, Network and System Sciences*, 9(7), 295-303.
19. Jamin, A.; and Mahonen, P. (2005). Wavelet packet modulation for wireless communications. *Wireless Comunication and Mobile Journal*, 5(2), 18 pages.
20. Baro, M.; and Ilow, J. (2008). PAPR reduction in OFDM using wavelet packet pre-processing. *Proceedings of the 5th IEEE Consumer Communications and Networking Conference*. Las Vegas, United States of America, 195-199.
21. Daly, D.; Heneghan, C.; Fagan, A.; and Vetterli, M. (2002). Optimal wavelet packet modulation under finite complexity constraint. *Proceedings of the International Conference on Acoustics, Speeech and Signal Processing*. Orlando, Florida, United States of America, 2789-2792.
22. Erdol, N.; Bao, F.; and Chen, Z. (1995). Wavelet modulation: A prototype for digital communication systems. *Proceedings of the IEEE Southcon Conference*. Florida, United States of America, 168-171.
23. Wong, K.M.; Wu, J.; Davidson, T.N.; Jin, Q.; and Ching, P.-C. (2000). Performance of wavelet packet division multiplexing in impulsive and gaussian noise. *IEEE Transactions on Communications*, 48(7), 1083-1086.

24. You, M.; and Ilow, J. (2004). A multi-wavelet packet modulation in wireless communications. *Proceedings of the Canadian Conference on Electrical and Computer Engineering*. Niagara Falls, Ontario, Canada, 2367-2370.
25. Rajni, C.; and Sikri, G. (2017). Distinctive approach to design tree in wavelet packet based OFDM system. *Journal of Engineering Science and Technology Review*, 10(6), 16-20.
26. Nerma, M.H.M. (2013). *Utilization of dual tree complex wavelet transform in OFDM*: A new OFDM system based on DTCWT. Riga, Latvia: LAP Lambert Academic Publishing.
27. Nerma, M.H.M.; Kamel, N.S.; and Jagadish, V.J. (2009). *On DTCWT based OFDM: PAPR analysis*. Lecture notes on electrical engineering. Multi-carrier systems & solutions. Dordrecht, Netherlands: Springer Science & Business Media.
28. Nerma, M.H.M.; Kamel, N.S.; and Jagadish, V.J. (2009). An OFDM system based on dual-tree complex wavelet transform (DTCWT). *Signal Processing: An International Journal (SPIJ)*, 3(2), 14-26.
29. Nerma, M.H.M.; Kamel, N.S.; and Jagadish, V.J. (2009). Performance analysis of a novel OFDM system based on dual-tree complex wavelet transform. *Ubicc Journal*, 4(3), 813-822.
30. Nerma, M.H.M.; Kamel, N.S.; and Jagadish, V.J. (2012). Investigation of using dual tree complex wavelet transform to improve the performance of OFDM system. *Engineering Letters*, 20(2), 8 pages.
31. Nerma, M.H.M.; Kamel, N.S.;. and Jagadish, V.J. (2008). PAPR analysis for OFDM Based on DTCWT. *Proceedings of the Student Conference on Research and Development (SCOReD 2008)*. Johor, Malaysia, 4 pages.
32. Nerma, M.H.M.; Kamel, N.S.; and Jagadish, V.J. (2009). On DTCWT based OFDM: PAPR analysis. *Proceedings of the 7th International Workshop on Multi-Carrier Systems & Solutions (MC-SS 2009)*. Herrsching, Germany, 207-217.
33. Nerma, M.H.M.; Kamel, N.S.; and Jagadish, V.J. (2009). BER performance analysis of OFDM System based on dual-tree complex wavelet transform in AWGN channel. *Proceedings of the 3rd WSEAS of the International Symposium on Wavelets Theory and Applications in Applied Mathematics, Signal Processing and Modern Science*. Istanbul, Turkey, 85-89.
34. Nerma M.H.M.; Jagadish, V.J.; and Kamel, N.S. (2010). The effects of HPA on OFDM system based on dual-tree complex wavelet transform (DTCWT). *Proceedings of the International Conference on Intelligent & Advance Systems*. Manila, Philippines, 1-4.
35. Nerma, M.H.M.; Jagadish, V.J. and Kamel, N.S. (2012). The effects of shift-invariance property in DTCWT-OFDM System. *Proceedings of the International Conference on Innovations in Information Technology*. Abu Dhabi, United Arab Emirates, 17-21.
36. Han, S.H.; and Lee, J.H. (2005). An overview of peak-to-average power ratio reduction techniques for multicarrier transmission. *IEEE Wireless Communications*, 12(2), 56-65.
37. Daoud, O.; Hamarsheh, Q.; and Damati, A. (2017). Papr effect remedy in OFDM-based wireless systems. *Journal of Communications Technology and Electronics*, 62(10), 1122-1129.

38. Ramjee, P. (2004). *OFDM for wireless communication systems*. Norwood, Massachusetts: Artech House.
39. Anoh, K.; Ikpehai, A.; Rabie, K.; Adebisi, B.; and Popoola, W. (2018). PAPR reduction of wavelet-OFDM systems using pilot symbols. *Proceedings of the International Symposium on Power Line Communications and its Applications*. Manchester, United Kingdom, 1-6.
40. Candes, E.J.; and Donoho, D.L. (2000). Curvelets-a surprisingly effective nonadaptive representation for objects with edges. *Proceeding of the Saint-Malo*. France, 1-10.
41. Choi, M.; Kim, R.Y.; Nam, M.-R.; and Kim, H.O. (2205). Fusion of multispectral and panchromatic satellite images using the curvelet transform. *IEEE Geoscience and Remote Sensing Letters*, 2(2), 136-140.
42. Ma, J.; and Plonka, G. (2007). Combined curvelet shrinkage and nonlinear anisotropic diffusion. *IEEE Transactions on Image Processing*, 16(9), 2198-2206.
43. Starck, J.-L.; Candes, E.J.; and Donoho, D.L. (2002). The curvelet transform for image denoising. *IEEE Transactions on Image Processing*, 11(6), 670-684.
44. Starck, J.-L.; Murtagh, F.; Candes, E.J.; and Donoho, D.L. (2003). Gray and color image contrast enhancement by the curvelet transform. *IEEE Transactions on Image Processing*, 12(6), 706-717.
45. Tessens, L.; Pizurica, A.; Alecu, A.; Munteanu, A.; and Philips, W. (2008). Context adaptive image denoising through modeling of curvelet domain statistics. *Journal of Electronic Imaging*, 17(3), 1-17.
46. Douma, H.; and de Hoop, M.V. (2007). Leading-order seismic imaging using curvelets. *Geophysics*, 72(6), S231-S248.
47. Hennenfent, G.; and Herrmann, F.J. (2006). Seismic denoising with nonuniformly sampled curvelets. *Computing in Science and Eng*ineering, 8(3), 16-25.
48. Shan, H.; Ma, J.; and Yang, H. (2009). Comparisons of wavelets, contourlets, and curvelets for seismicdenoising. *Journal of Applied Geophysics*, 69(2), 103-115.
49. Bermejo-Moreno, I.; and Pullin, D.I. (2008). On the non-local geometry of turbulence. *Journal of Fluid Mechanics*, 603, 101-135.
50. Farge, M.; Pellegrino, G.; and Schneider, K. (2001). Coherent vortex extraction in 3D turbulent using orthogonal wavelets. *Physical Review Lett*ers, 87(5), 054501.
51. Ma, J.; and Hussaini, M.Y. (2007). Three-dimensional curvelets for coherent vortex analysis of turbulence. *Applied Physics Letters*, 91(18), 184101-184101-3.
52. Ma, J.; Hussaini, M.Y.; Vasilyev, O.V.; and Le Dimet, F.-X. (2009). Multiscale geometric analysis of turbulenceby curvelets. *Physics of Fluids*, 21(7), 075104.
53. Candes, E.J.; and Demanet, L. (2003). Curvelets and fourier integral operators. *Comptes Rendus Mathematique*, 336(5), 395-398.
54. Candes, E.J.; and Demanet, L. (2005). The curvelet representation of wave propagators is optimally sparse. *Communication on Pure and Applied Mathematics*, 58(11), 1472-1528.

55. Candes, E.J.; Romberg, J.; and Tao, T. (2005). Stable signal recovery from incomplete and inaccurate information. *Communication on Pure and Applied Mathematics*, 59, 1207-1233.
56. Candes, E.J.; and Tao, T. (2206). Decoding by linear programming. *IEEE Transactions on Information Theory*, 51(12), 4203-4215.
57. Donoho, D. (2006). Compressed sensing. *IEEE Transactions on Information Theory*, 52(4), 1289-1306.
58. Herrmann, F.J.; and Hennenfent, G. (2008). Non-parametric seismic data recovery with curvelet frames. *Geophysical Journal International*, 173(1), 233-248.
59. Herrmann, F.J.; Moghaddam, P.; and Stolk, C.C. (2008). Sparsity-and continuity-promoting seismic image recovery with curvelet frames. *Applied and Computational Harmonic Analysis*, 24(2), 150-173.
60. Candes, E.J.; Demanet, L.; Donoho, D.L.; and Ying, L. (2006). Fast discrete curvelet transforms. *Multiscale Modeling and Simulation*, 5(3) 861-899.
61. Duijndam, A.J.W.; and Schonewille, M.A. (1999). Nonuniform fast fourier transform. *Geophysics*, 64(2), 539-551.